

# Diffusion tensor imaging and micro-computed tomography based three dimensional stereotaxic atlas of the adult C57BL/6J mouse brain corrected for postmortem tissue deformation

M. Aggarwal<sup>1</sup>, J. Zhang<sup>2</sup>, M. I. Miller<sup>1,3</sup>, and S. Mori<sup>2,4</sup>

<sup>1</sup>Department of Biomedical Engineering, Johns Hopkins University School of Medicine, Baltimore, MD, United States, <sup>2</sup>Department of Radiology, Johns Hopkins University School of Medicine, Baltimore, MD, United States, <sup>3</sup>Center of Imaging Science, Johns Hopkins University, Baltimore, MD, United States, <sup>4</sup>F. M. Kirby Research Center for Functional Brain Imaging, Kennedy Krieger Institute, Baltimore, MD, United States

**Introduction:** Stereotaxic atlases of the mouse brain play an important role in neuroscience research for targeting specific brain structures during surgical operations. Stereotaxic surgery relies on determining the precise coordinates of brain structures based on external skull landmarks. Existing atlases offering stereotaxic coordinates of the mouse brain are mostly histology based<sup>1</sup>. Several groups have developed MRI based population averaged mouse brain atlases that offer improved precision<sup>2,3</sup>. However, since MRI has limited value for visualizing skull structures, these atlases are not in the stereotaxic coordinate frame. Recently, the first micro-computed tomography (microCT) and MRI combined stereotaxic atlas of the adult mouse brain<sup>4</sup> was published. We have previously used high resolution diffusion tensor imaging (DTI) to develop microCT-DTI based mouse brain atlases at six developmental ages<sup>5</sup>. While these MRI based atlases have high contrast and SNR, the morphological fidelity to *in vivo* mouse brains has not been evaluated. In order to account for a) anatomical variability in the brain, and b) tissue postmortem distortion due to fixation, we developed a population-averaged *in vivo* MRI template of the adult C57BL/6J brain with estimates of variability; and a distortion corrected high resolution DTI atlas was developed by nonlinear mapping of the *ex vivo* data to the population averaged *in vivo* template. The distortion corrected atlas was incorporated into the stereotaxic coordinate frame. Compared to commonly used histology atlases, our distortion corrected DTI atlas in stereotaxic coordinates provides a more accurate representation of mouse brain anatomy. The atlas contains high contrast and high fidelity views of brain anatomy with CT and multiple MRI contrasts (T2-w, diffusion-weighted, anisotropy and orientation maps), and can serve as an important resource for increasing the precision of stereotaxic operations in the adult mouse brain.

**Methods:** *In vivo* MRI of 9 adult brains was done on a 9.4T spectrometer, using a 3D T2-w fast spin echo (FSE) sequence with navigator echo phase correction (ETL = 4, TE/TR = 35/700 ms, NA = 2, scan time = 1 h). The spectral data were zero-filled to give a resolution of 50 x 50 x 125  $\mu\text{m}^3$ . 5 of these samples were imaged for all CT, *in vivo* and *ex vivo* MRI. DTI of *ex vivo* intracranially-fixed brains was done on an 11.7T scanner using a 3D diffusion-weighted multiple spin echo sequence (ETL = 4, TE/TR = 35/550 ms, NA = 2,  $b = 1600-1800 \text{ s/mm}^2$ , 6 diffusion directions, scan time = 24h). The nominal resolution after zero-filling was 62.5 x 62.5 x 62.5  $\mu\text{m}^3$ . T2-w images were acquired with the same field-of-view and resolution (3D FSE sequence, ETL = 4, TE/TR = 40/800 ms, NA = 4, scan time = 4 h). MicroCT was done on a SkyScan 1172 system at an isotropic resolution of 18  $\mu\text{m}$  (70 kV/141  $\mu\text{A}$ , 0.4° step, 158 ms exposure time). The CT skull and MR brain images of each mouse were coregistered using landmark-based rigid registration as described previously<sup>5</sup>. To create the population averaged atlas, all *in vivo* brain images were intensity-normalized and rigid aligned to one brain chosen as the reference. The aligned images were voxel-wise intensity-averaged to create the first population-averaged brain (R1). Using R1 as the template, the aligned images were affine (12-mode linear) transformed, and averaged to generate the second reference (R2). R2 was then used as the new template for affine transformation. This process was iterated 4 times to generate the fourth reference (R4). Finally, all *in vivo* images were nonlinearly deformed to R4 by Large Deformation Diffeomorphic Metric Mapping (LDDMM)<sup>6</sup>, and averaged to create the final population-averaged *in vivo* atlas. The deformation maps record the differences between each brain and the template. By averaging the magnitude of the deformation vectors at each voxel, an anatomical variability magnitude (AVM) map was created. To place the *in vivo* averaged atlas in stereotaxic coordinates, the CT skull images from the 5 mice were registered at the bregma (after bregma-lambda horizontal alignment). The bregma aligned *in vivo* brain images of these mice were then superimposed and averaged, and used as the reference to rigid align the population averaged *in vivo* atlas. To measure the shrinkage due to fixation, the linear dimensions and total volume of brain tissue were computed from the *in vivo* and *ex vivo* T2-w images of each animal. To correct for tissue shrinkage, the *in vivo* population averaged atlas was used to warp an *ex vivo* T2-w image nonlinearly using LDDMM. The resultant transformation was applied to the diffusion tensor to generate a high resolution DTI atlas in the stereotaxic coordinate frame.

**Results & Discussion:** Fig. 1A shows a section from the population-averaged *in vivo* adult brain template, which was generated by the procedure described above, to be unbiased and to represent the 'average' anatomy within the sample population. The AVM map, showing the average inter-animal variability within the brain is shown in Fig. 1B. Grey scale intensities in the AVM represent distances in micrometers. The highest degree of variability across animals, upto 0.21 mm, was seen in the brainstem and nose bulb regions. Tissues around the lateral ventricles also tended to have high variability (upto 0.16 mm). The average spatial variability of the entire brain was calculated to be 0.10 mm. The total brain tissue volume was observed to be  $472.8 \pm 11.6 \text{ mm}^3$  for *in vivo* brains, and  $454.4 \pm 12.5 \text{ mm}^3$  for *ex vivo* brains (indicating 3.9% average volumetric shrinkage). Fig. 1C shows the shrinkage distortion corrected high resolution DTI brain atlas, after nonlinear deformation to the population-averaged *in vivo* template using LDDMM, embedded in the population-averaged skull data from microCT. Coronal sections from direction-encoded color (DEC) maps derived from DTI are also shown. The quality of the distortion correction is illustrated by superimposing the contours for the brain and ventricle volumes from the *in vivo*

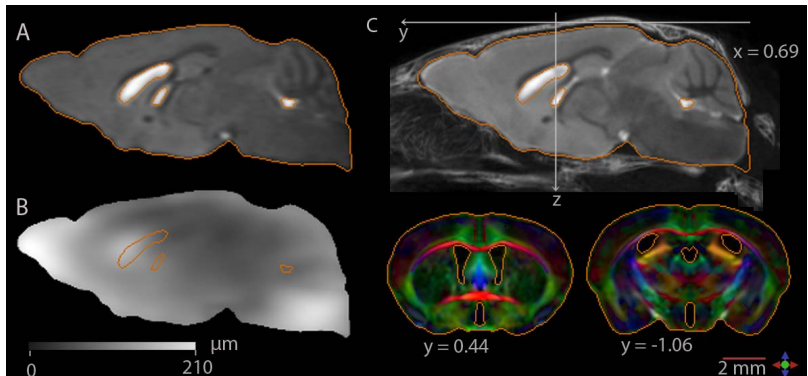


**Fig. 1:** The shrinkage-corrected CT-DTI atlas. **A)** Section from the population-averaged *in vivo* T2-w template of adult C57BL/6J brain. **B)** AVM map of the section in A. **C)** Shrinkage-distortion corrected *ex vivo* DTI atlas in stereotaxic coordinates. Top) a T2-w brain sagittal section with the averaged CT images of 5 bregma-aligned skulls overlaid, and Bottom) DEC coronal sections. Crosshairs denote the location of the bregma landmark, all coordinates are specified with respect to bregma as the origin.

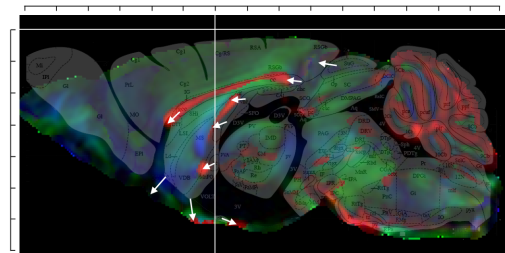


**Fig 2:** Tissue distortion in histology-based atlas revealed by comparing the mid-sagittal section from the Paxinos atlas and corresponding DEC map from the shrinkage-corrected CT-DTI atlas. Crosshairs mark the location of the bregma. Scale is in units of mm.

template onto the distortion corrected *ex vivo* image. Fig. 2 shows a comparison of the shrinkage distortion corrected CT-MRI stereotaxic atlas with the Paxinos atlas of the adult C57BL/6J brain. The alignment of the atlases was better in the caudal (brainstem and cerebellum) areas. White arrows indicate the shifted locations of structures in the interior of the brain (anterior commissure, genu and splenium of corpus callosum) by about 0.4 mm in the CT-MRI atlas as compared to the histology based atlas. A 3D viewing software 'AtlasView' was used to provide user-interface for navigation through the different imaging contrasts and specification of stereotaxic coordinates of any location within the brain.

**References:** [1] Paxinos & Franklin, *Acad Press* 2001. [2] Badea *et al*, *Neuroimage* 37, 2007. [3] Dorr *et al*, *Neuroimage* 42, 2008. [4] Chan *et al*, *Neuroscience* 144, 2007. [5] Aggarwal *et al*, *ISMRM* 2007. [6] Miller *et al*, *Ann Rev Biomed Eng* 4, 2002.